Soft Computing (2019) 23:3449–3463
https://doi.org/10.1007/s00500-017-3002-z

METHODOLOGIES AND APPLICATION

Bio-inspired heuristics for layer thickness optimization in multilayer piezoelectric transducer for broadband structures

Aneela Zameer[1] · Mohsin Majeed[2] · Sikander M. Mirza[3] · Muhammad Asif Zahoor Raja[4] · Asifullah Khan[1] · Nasir M. Mirza[3]

Published online: 13 January 2018

Abstract
Recently, enhancement of sensitivity of multilayered piezoelectric transducer and reduction in electrical impedance has gained importance due to development of stacked active element designs. This work presents mathematical optimization of layer thicknesses for broadband structures using piezo-composite with ceramic and single crystal as active material for underwater SONAR. The proposed technique employs bio-inspired heuristics-based genetic algorithms by invoking one-dimensional thickness model. Initially, optimization has been performed for monolithic materials in the stack for various acoustic media, and then, the results were validated by comparing with the published data. In the proposed scheme, optimization is carried out for two-phase 1–3 piezo-composite stacks with same active elements for better mechanical output and broadband structure while preserving the minima among first three harmonics under -3 and -6 dB from the peaks in the frequency spectrum. The results show that the optimized single-crystal-based transducers have higher mechanical output and lower electrical impedance than their counterparts using piezo-ceramic in single- and two-phase materials.

Communicated by V. Loia.

✉ Aneela Zameer
aneelaz@pieas.edu.pk; aneelas@gmail.com

Mohsin Majeed
mohsinmajeed08@gmail.com

Sikander M. Mirza
sikander@pieas.edu.pk

Muhammad Asif Zahoor Raja
rasifzahoor@yahoo.com

Asifullah Khan
asif@pieas.edu.pk

Nasir M. Mirza
nmm@pieas.edu.pk

[1] Department of Computer and Information Sciences, Pakistan Institute of Engineering and Applied Sciences (PIEAS), Nilore, Islamabad 45650, Pakistan

[2] Department of Nuclear Engineering, Pakistan Institute of Engineering and Applied Sciences (PIEAS), Nilore, Islamabad 45650, Pakistan

[3] Department of Physics and Applied Mathematics, Pakistan Institute of Engineering and Applied Sciences (PIEAS), Nilore, Islamabad 45650, Pakistan

[4] Department of Electrical Engineering, COMSATs Institute of Information Technology, Attock Campus, Attock, Pakistan

Graphical abstract

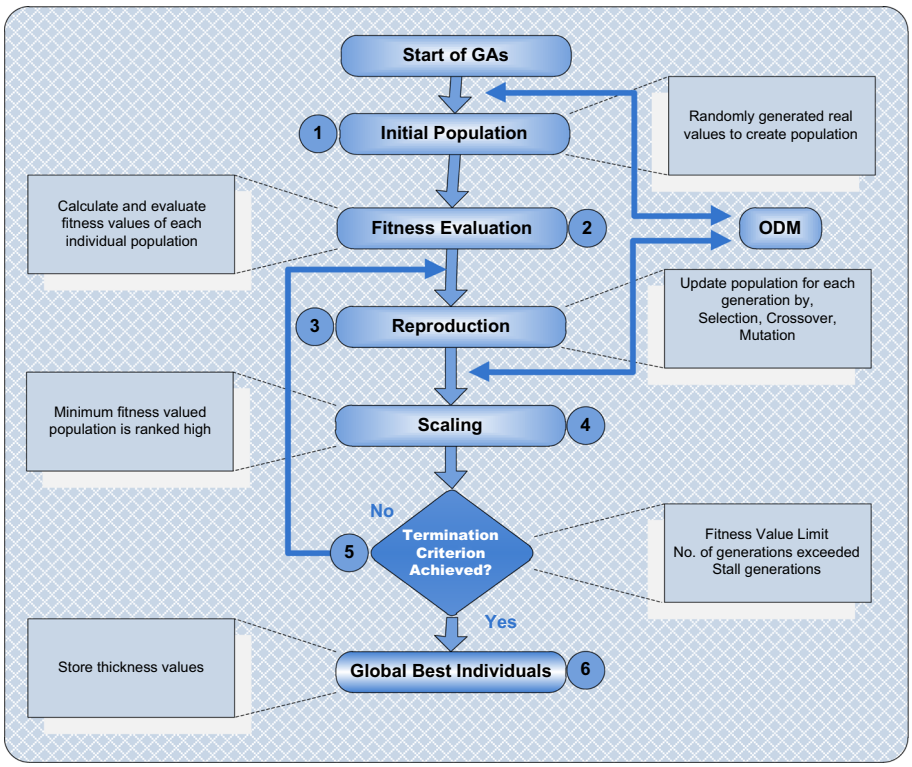

Keywords Genetic algorithms · Piezo-ceramic transducer · SONAR · Piezo-composites · Single crystal · Optimization

1 Introduction

Exploration and exploitation of multilayers transducers for higher sensitivity and reduced electrical impedance, is the potential area of research for the development of stacked structures. Classically, there have been three stages in the development of piezoelectric materials. In the first phase, ferroelectric materials including quartz and barium titanate were used. In the second stage, piezoelectric ceramic materials, e.g., lead zirconate titanate (PZT) were employed. In the last phase, the most advanced form of piezoelectric materials composed of single crystals is developed, e.g., lead magnesium niobate–lead titanate (PMN-PT), for exhaustive use in ultrasonic transducers. Along with the development of piezoelectric materials, ultrasonic transducer manufacturing has been revolutionized devising broad applications in various fields including sound navigation and ranging (SONAR), physical acoustics, medical ultrasonics, nondestructive testing and evaluation, sono-chemistry and material characterization (Soloviev et al. 2016; Mattiat 2013). Piezoceramic- and piezo-composite material-based structures have been studied for energy harvesting (Soloviev et al. 2016), nano-positioning devices (Ru et al. 2015), concrete crack damage location (Xu et al. 2015), medical ultrasound (Martin et al. 2014), and many others (Mokrý 2016).

For better utilization of transducers, optimization has been performed for some specific applications for maximizing sensitivity and coupling constants, and minimizing the input to the ultrasonic transducer. Constrained and unconstrained problems are solved by exploiting the competency of evolutionary and swarm optimization techniques in diverse fields of science and engineering (Abo-Hammour et al. 2013; Liu et al. 2017; Chen et al. 2017; Jurczuk et al. 2017; Abo-Hammour et al. 2014a). Specially, in the field of ultrasonics few significant application of these methodologies include (Fu et al. 2006); they performed multi-objective optimization by using Pareto-based multi-objective evolutionary algorithm to maximize the mechanical output in terms of pressure amplitude and minimize the input to the ultrasonic transducer. Ruíz et al. (2004) used genetic algorithms (GAs) to ascertain the optimum internal design parameters such as thickness and acoustic impedance for existing piezoelectric ultrasound transducers. Many researchers have studied uniform multiple layers of the active material of a transducer. The improved design of ultrasonic transducer is developed in terms of higher sensitivity and electromechanical coupling constant (Rhim et al. 2004). However, for non-uniform multiple layers, there are only a few attempts to optimize such design. Among them, Abrar and Cochran (2007) worked on non-uniform multiple active layers by using simulated

annealing (SA) technique. The same stochastic technique has also been implemented by others for weighting and thinning of wide-band arrays (Lommi et al. 2002).

The prime purpose of present work is to make use of the capability of generating output on even harmonics, in the form of an optimized transducer by varying layer thicknesses for broadband structures. For such an optimized design for higher mechanical output and broadband, mathematical optimization has been conducted by employing genetic algorithms for single-phase and two-phase transducers, and results are validated. Materials used for such a design optimization are piezo-ceramic and single crystal along with their composites with polymers. It is worth mentioning here that single-crystal-based composite transducers have been optimized first time for better mechanical output. Furthermore, it can be demonstrated that the robustness without trapping in local minima and parallel search capability make GAs more attractive and suitable as an optimization mechanism. For vast range of applications it is required to design such a transducer that can operate at a relatively smaller value of operating voltage, low frequency and high sensitivity.

Optimization of multiple layer thicknesses arises from the fact that by increasing number of active layers to N in a transducer which is electrically connected in parallel and mechanically in series, the electrical impedance decreases by $1/N^2$ in contrast to single-layered transducer of same total thickness. Similarly, in case of transmission, mechanical output (in terms of pressure magnitude) increases by a factor of number of layers (N) for an applied electrical voltage due to the increase in capacitance of multiple-layered ceramic. Furthermore, the design flexibility is also achieved by employing more than one active layers (Abrar and Cochran 2007). In this work, piezoelectric materials studied include PZT5H and single crystal, PMN-PT and their 1–3 composites with epoxy CY1301/HY1300 as passive element. Their responses in various loading media are also analyzed. It is the first time that optimization is carried out for single-crystal material-based piezo-composite multilayer transducer design by varying layer thicknesses using genetic algorithms (GAs). The contribution is summarized in terms of salient features of the present study as listed below:

- Multiple-layered piezoelectric structures give response on even harmonics when layer thicknesses are non-uniform, which are optimized for higher values of the mechanical output by varying individual layer thicknesses exploiting bio-inspired heuristics-based genetic algorithms and its comparison with particle swarm optimization and the simulated annealing techniques.
- The strength of genetic algorithms evolutionary computing technique has been utilized for better exploration of optimized transducer design than its counterparts.
- Provision of flexibility to extend optimization of single-crystal-based structures effectively by exploiting GAs result in design of optimized single-crystal-based structure yields broader values of bandwidth as compared to piezo-ceramic- and piezo-composite-based materials in multilayer transducers.
- Smooth trouble-free implementation, simplicity of the concepts and inherent robust nature of the algorithm lead to effective and reliable transducer design.

The organization of this paper is as follows: Sect. 2.1 consists of one-dimensional modeling of the transducer. Here, mathematical expressions, scope and limitations of one-dimensional model (ODM) are discussed. Methodology of using genetic algorithms in the present scenario of case study is also presented. Section 2.2 discusses optimization process for the design of both piezoelectric ceramic and composite transducers. Section 3 deals with results and discussion of optimized designs of single- and two-phase transducers. The conclusions are presented in Sect. 4.

2 Material and methods

In this section, the proposed methodology is presented which consists of brief overview of system model, ODM and optimization mechanics comprising of formulation of fitness function, optimization with GAs, procedural steps and computational flow diagram.

2.1 One-dimensional model mathematical formulation

One-dimensional model of ultrasonic transducer is primarily based on solution of unidimensional wave equation by exploiting matrix operations. ODM assumes that the lateral dimensions (width and length) of ultrasonic transducer are considerably larger than thickness direction and the generated ultrasound waves are propagating along the thickness dimension in the form of longitudinal plane waves.

The constitutive equations representing plane compressional waves propagating in the thickness (z-direction) of a piezoelectric layer are:

$$S = s_{\mathrm{E}} \cdot T + d^t \cdot E, \tag{1}$$

$$D = d \cdot T + \varepsilon_T \cdot E. \tag{2}$$

For single layer, Eqs. (1) and (2) can be written in differential equation form with variable z (indicating transducer thickness dimension) as:

$$T = c\frac{\partial \psi}{\partial z} - hD \tag{3}$$

Table 1 List of symbols

S	Mechanical strain vector
s_E	Compliance coefficient matrix at constant or zero electric field
T	Mechanical stress vector
d^t	Strain constants matrix at constant or zero strain
E	Electric field vector
ε_T	Relative permittivity at constant or zero strain
D	Electric charge density vector
ψ	Particle displacement (m)
v	Particle velocity (m/s)
ε	Relative dielectric constant
ε_0	Dielectric constant of free space
A	Cross-sectional area of the transducer
t	Thickness of piezoelectric material

$$E = -h\frac{\partial \psi}{\partial z} + \frac{D}{\varepsilon} \tag{4}$$

Using Eqs. (3) and (4) along with Newton's second law of motion, we get one-dimensional wave equation as:

$$\frac{\partial^2 \psi}{\partial t^2} = v^2 \frac{\partial^2 \psi}{\partial z^2} \tag{5}$$

where,

$$v^2 = \frac{k}{\rho} \tag{6}$$

The symbols used are defined in Table 1. The one-dimensional model (ODM) is mainly developed on solving wave equation in terms of matrix-based solution. The inverse Fourier transform (IFT) analysis is carried out over a broad frequency range to execute time-domain analysis (Powell et al. 1998). ODM is thus analogous to linear systems formulation. A computer program is developed covering ODM comprises of following steps:

Step 1 *Pre-processing* Geometrical forms, materials, physical and numerical parameters along with equivalent electric circuitry of transducer are used as input to the code.

Step 2 *Processing* ODM is employed for the solution of 1-D wave equation through matrix operation and manipulation.

Step 3 *Post-processing* Output from the transducer in transmission mode is collected in terms of electrical impedance and acoustic pressure.

The ODM has already been validated by detailed experimental investigations (Wu et al. 2003; Cochran et al. 2005) as well as by exploiting PZ Flex (a time-domain finite element analysis program) by Abrar and Cochran (2007). The ODM can extensively be used for several active and/or passive layers, backing layer, matching layer(s), front and back loading, and external electrical circuit, for piezoelectric transducers. A quick simulation can be executed to understand the general performance of a transducer. ODM is equally efficient to model transmitters and receivers; however, it does not consider lateral modes; therefore, it is unable to estimate resonance activity in this direction. A diagram of three-layered stacked transducer is demonstrated in Fig. 1. In this case, three layers are mechanically connected in series but electrically in parallel. Polarity of consecutive layers is oppositely directed along thickness.

Present work considers transucer in transmission mode with the main focus on the study of piezoelectric materials in multilayer transducers keeping rest of components

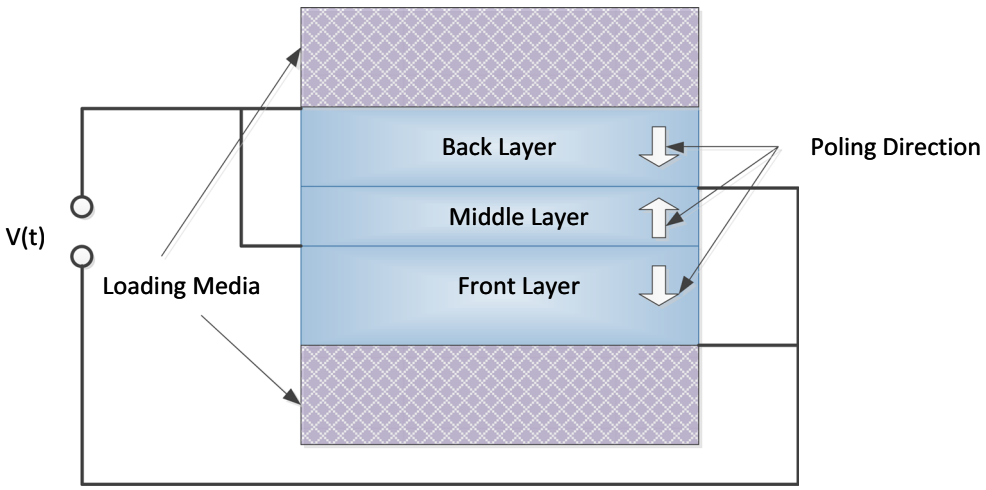

Fig. 1 Schematic representation of a three-layered transducer

unchanged. Only resistive load of the transducer is considered, while reactive load (capacitance and inductance) is typically negligible.

2.2 Proposed GA-based layer thickness optimization strategy

After the induction of genetic algorithms by Holland in early 1970s with motivation of theory of evolution, bio-inspired computing framework-based GA has been implemented in diverse fields of nanotechnology (Raja 2014a), fuel ignition model (Raja 2014b), electrical conducting solids (Raja et al. 2016a), automatic control (Panda and Yegireddy 2013), thin film flow (Raja et al. 2015b), digital communications (Dey et al. 2014), electromagnetic theory (Khan et al. 2015a), nuclear reload pattern optimization (Zameer et al. 2014), magneto-hydrodynamics (Raja 2014c), economic and financial mathematics (Abo-Hammour et al. 2014b), solving singular differential equations (Hochreiter and Waldhauser 2015), election night forecast (Paul et al. 2015), traveling salesman problem (Gao and Ovaska 2002), and motor fault detection (Berlincourt et al. 2000). These factors motivated authors to select GA as an optimization mechanism to solve system model. The flow diagram of optimization process is shown in Fig. 2. The process has the following pseudocode of GA for optimal transducer design:

Step 1 *Initial population* Starting with the initial randomly generated population of chromosomes, a randomly generated set of three-layered thicknesses is selected and normalized to the total thickness, which is then input into ODM.

Step 2 *Fitness evaluation* The optimization methodology has been implemented in a MATLAB control program. This program extracts figures of interest from the mechanical output files from ODM (e.g., peak values of pressure output curve) and then calculates the fitness function for the current iteration.
Following is the fitness function that GA uses to minimize it in successive generations.

$$O_{\text{fsp}} = \frac{(P_1 - P_2)^2}{(P_1 + P_2)^2} + \frac{(P_2 - P_3)^2}{(P_2 + p_3)^2} + \frac{(P_3 - P_1)^2}{(P_3 + P_1)^2} \tag{7}$$

where O_{fsp} is the fitness function of single-phase transducer and P_k is the output pressure magnitude (Pa) at the kth harmonic frequency. This fitness function is used to measure the maximized uniformity of initial three harmonics quantitatively for single-phase transducers. However, for two-phase transducers, the objective function for the optimization of

$$O_{\text{ftp}} = \frac{1}{P_{\text{c}}^{*}\text{BW}_{-3\,\text{dB}}} \tag{8}$$

where O_{ftp} is the fitness function for two-phase transducers, P_{c} is the pressure at central frequency, and $\text{BW}_{-3\,\text{dB}}$ is the bandwidth relative -3 dB bandwidth.

Step 3 *Reproduction* to produce next generation of competitive survivors, GA employs reproduction process, which comprises of three sub-processes: selection, crossover and mutation. Graphical overview of reproduction is presented in Fig. 2b.
Selection It makes fitness base selection of chromosomes for the recombination required for producing a population of next generation. Recombination consists of crossover between the parents and mutation within a chromosome.
Crossover It selects genes from the pair of current individuals and combines them to produce new offspring (or solution).
Mutation GA makes random changes in the genes of an individual to make a new child. It avoids to be trapped in local minima by using mutation.

Step 4 *Fitness evaluation* the freshly generated population undergoes evaluation process according to fitness values computed through Eq. 5, and hence, selection of individuals takes place on the basis of best fitness value for next step.

Step 5 *Scaling* It transforms raw fitness values achieved so far into values within a range appropriate for the selection criterion.

Step 6 *Termination* Once scaling is performed, execution process between steps 3 and 5 keeps going unless one of the stopping criteria is met. The algorithm stops when the maximum number of generations is met, the fitness achieved in any generation is equal to or smaller than the required fitness value, or fitness value does not improve for a prescribed generation number.

Next generation is selected on the basis of reproduction of parents with best fitness values along with newly generated offspring. This iterative process produces successive generations with enhanced fitness values. Therefore, GA avoids getting trapped in local minima of the optimization problem (McCall 2005). The initial assignments and declarations for the various parameters of GA are illustrated in Table 2.

For effective optimization, independent executions of GAs optimizer are carried out with different reproduction operators. Some variants of GAs are selected as listed in Table 3 as employed in (Raja et al. 2015a); present optimization problem has linear constraint as total thickness of transducer is kept 1 mm for single-phase and 3 mm for two-phase transduc-

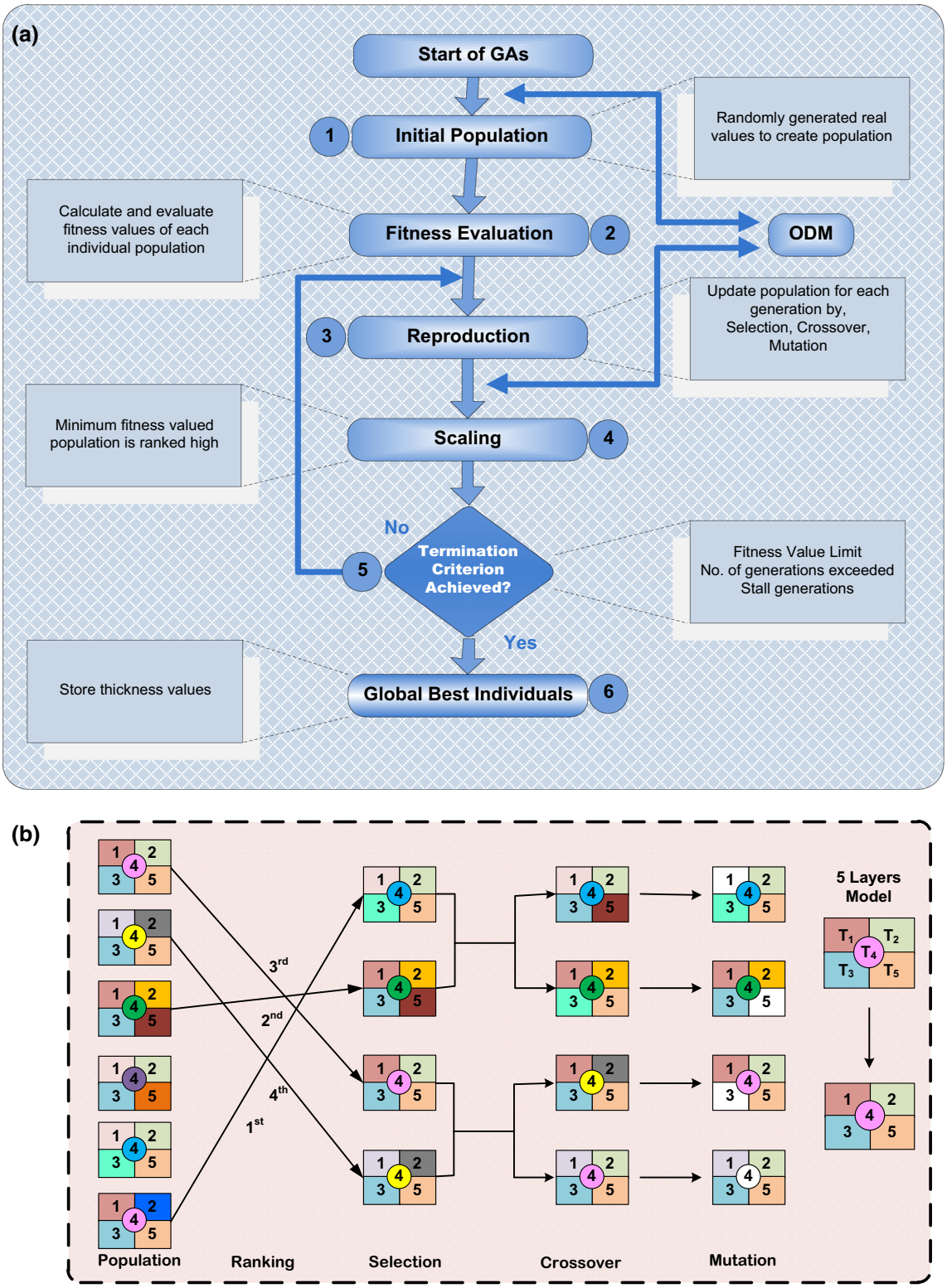

Fig. 2 Design methodology of genetic algorithm-based transducer optimization **a** overall flow diagram and **b** graphical overview of reproduction mechanism of GAs

Table 2 Parameter settings for GAs in simulations

Parameter	Value
Population creation	Linear feasible
Population size	Various values
Generations	50
Stall generations	20
Scaling fraction	Rank
Ratio	1.25
TolFun	10^{-9}
TolCon	10^{-9}
Elite count	2
Crossover fraction	0.8

Table 3 GA variants employed in this work (Hochreiter and Waldhauser 2015)

Methods	Selection	Crossover	Mutation
GA1	Stochastic uniform	Heuristic	Adaptive feasible
GA2	Stochastic uniform	Arithmetic	Adaptive feasible
GA3	Remainder	Heuristic	Adaptive feasible
GA4	Remainder	Arithmetic	Adaptive feasible
GA5	Roulette	Heuristic	Adaptive feasible
GA6	Roulette	Arithmetic	Adaptive feasible

ers; therefore, Table 3 is used for the simulations in selecting the GA variants.

3 Results and discussion

The ultrasonic transducer model developed in this work has been validated by comparing the currently predicted values exploiting GAs with the corresponding values found in the reported data implemented simulated annealing (SA) (Abrar and Cochran 2007). The optimization code developed with GAs and making use of ODM for each fitness evaluation has been executed. Two types of piezoelectric ultrasound transducers are studied. In the first case, single-phase transducer with piezo-ceramic (PZT5H) and single-crystal (PMN-PT) materials is used. In the other case two-phase transducers, i.e., combination of these piezo-ceramic or single-crystal materials with polymer making composite transducers, are employed. In order to study the characteristics of these materials, simple ODM is used excluding details such as backing layer, matching layer and bond lines. The corresponding results are presented in the following subsections.

3.1 Analysis of single-phase transducer

Two different piezoelectric materials have been used: piezo-ceramic lead zirconate titanate (PZT5H) and single-crystal lead magnesium niobate–lead titanate (PMN-PT). PZT5H has been selected from PZT family because PZT5H has the highest sensitivity and high permittivity in PZT family; it has widely been used in piezoelectric transducers. The relaxor-based ferroelectric materials have revolutionized the field of piezoelectric transducers. Particularly PMN-PT has been greatly in use in preparing ultrasonic transducer due to its enormous piezoelectric properties and ultra-bigger higher electromechanical coupling factor. Material properties of PZT5H and PMN-PT are presented in Table 4. The total thickness of transducer is kept 1 mm, and three active piezoelectric layers are incorporated.

Table 4 Material parameters for PZT5H and PMN-PT

Parameters	PZT5H	PMN-PT
Elastic stiffness, C_{11}^E (N m^{-2})	1.26×10^{11}	1.14×10^{11}
Elastic stiffness, C_{12}^E (N m^{-2})	7.95×10^{10}	1×10^{11}
Elastic stiffness, C_{13}^E (N m^{-2})	8.41×10^{10}	1.12×10^{11}
Elastic stiffness, C_{33}^E (N m^{-2})	1.17×10^{11}	1.29×10^{11}
Piezoelectric stress constant, $e31$ (cm^{-1})	-6.5	-3.4
Piezoelectric stress constant, $e33$ (cm^{-1})	23.3	19.6
Relative permittivity, ε_R^T	3400	8266
Relative permittivity, ε_R^S	1470	3026
Density, ρ (kg m^{-3})	7500	8050
Material attenuation, α (dB cm^{-1}, at 1 MHz)	0.08	1

3.1.1 Piezo-ceramic: PZT5H-based multilayer transducer

Simulations have been performed under various acoustic loading media. For air as acoustic coupling media, the optimization code has been executed and results are shown in Fig. 3 in the form of evolutionary progress plot from optimized transducer and output of the optimized forward transducer model in the form of pressure and impedance. It depends on the equipment for practical constraints, but to validate results the truncated values of thickness up to 1 μm were provided as input to ODM with the constraint of manufacturing tolerance of 10 μm. Figure 3a illustrates the evolution graph of fitness values versus the consecutive generations. It can be observed that the fitness value declines with generations. After carrying out 135 iterations while the six generations have been produced, the fitness value (3.86×10^{-6}) for the transducer design with air as acoustic media was found to be less than the fitness limit set as one of the termination criteria. The fitness limit was set as 1×10^{-5} for both single-phase and two-phase transducers.

The electrical impedance magnitude and phase are presented in Fig 3b, and pressure magnitude in Pa and dB is shown in Fig. 3c, d, respectively. The peak pressures of optimized transducer at first three harmonics achieved are closer

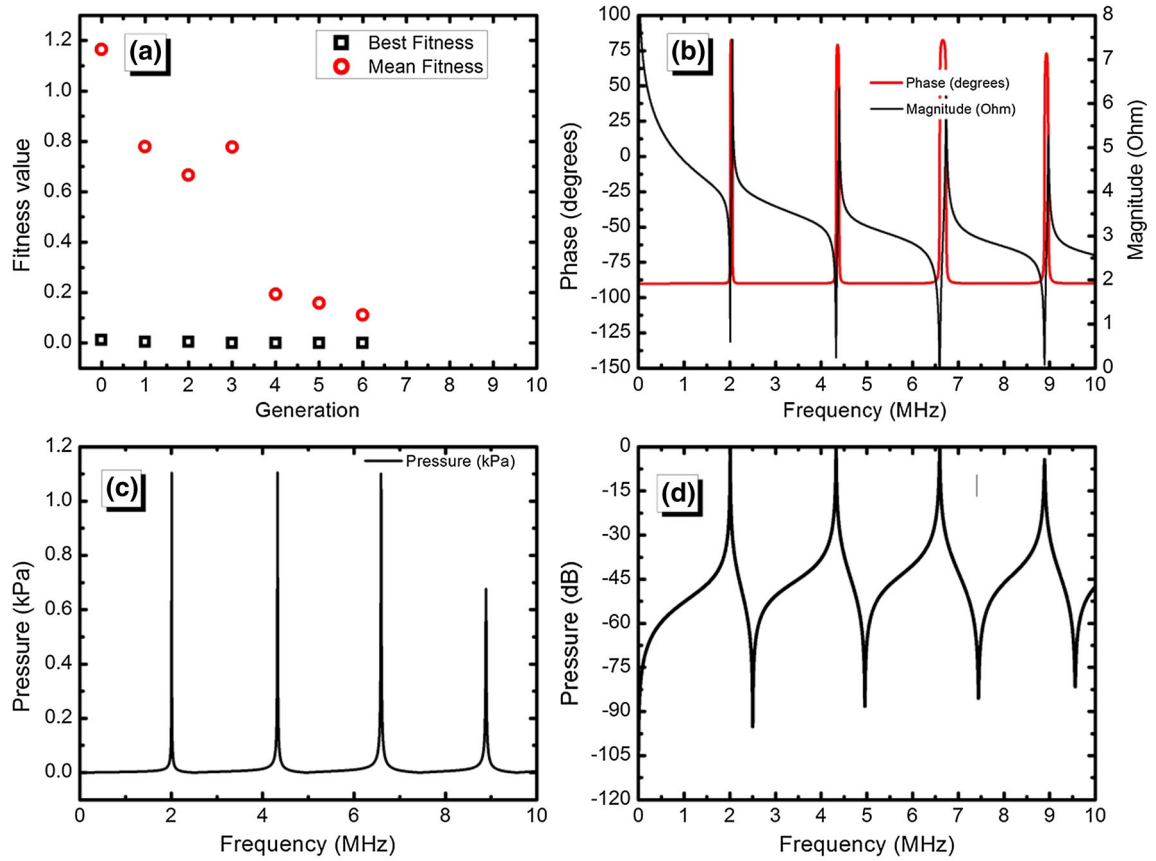

Fig. 3 Optimized three-layered PZT5H transducer results with air–air acoustic loading using GA. **a** Convergence of fitness function, **b** magnitude (Ω) and phase (°) of electrical impedance, and **c** output pressure (Pa) and **d** output pressure (dB)

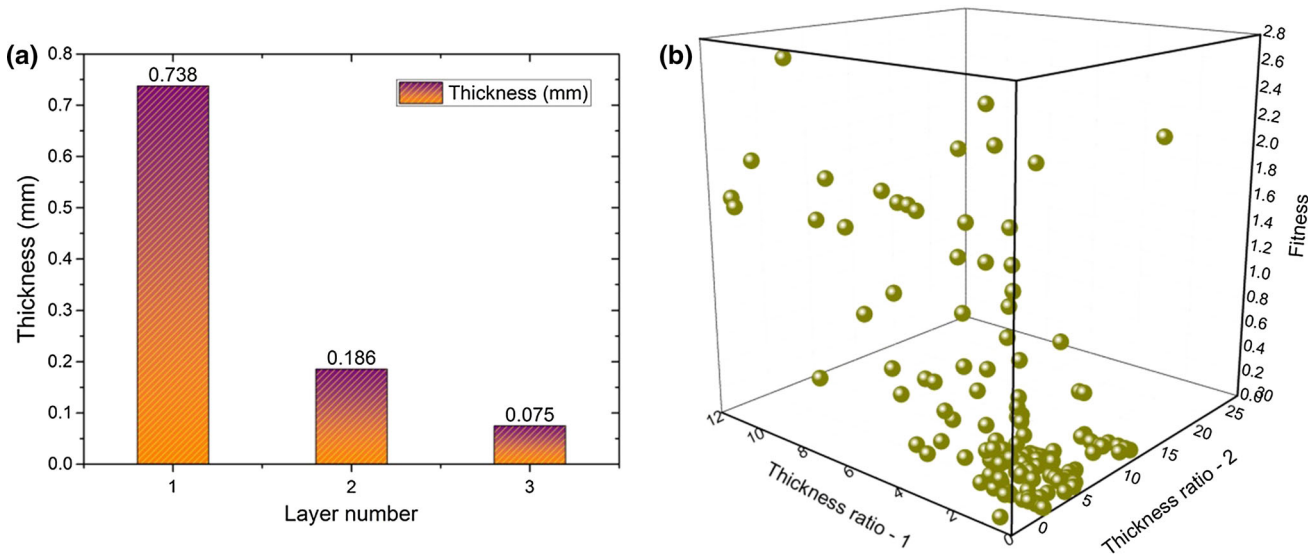

Fig. 4 **a** Layer thickness values and **b** layer thickness ratios of layers 1 and 2 w.r.t. layer 3 of the optimized transducer design by genetic algorithms (1 = back layer, 2 = middle layer, and 3 = front layer)

to 1105.04, 1105.78 and 1102.41 (all in Pa), respectively. It can be observed from the figure that the pressure peaks are quite close and uniform. The transducer thus is optimized with thickness values of 0.738, 0.186 and 0.075 mm, back to front, and shows maximum pressure magnitude around frequencies 2.01, 4.33 or 6.59 MHz. As seen from electrical

Table 5 Optimized results of layer thicknesses with variation of loading

Media (front–back)	Fitness value	Iteration count	Generation count	Layer thickness (mm)			GA variant
				T_1	T_2	T_3	
Air–air	9.1×10^{-6}	135	6	0.738	0.186	0.075	GA6
Air–water	2.8×10^{-6}	476	23	0.553	0.179	0.278	GA4
Water–epoxy	6.7×10^{-6}	896	44	0.563	0.184	0.280	GA6
Water–air	1.7×10^{-6}	275	13	0.589	0.175	0.238	GA1

Table 6 Comparison of optimization results with GA, PSO and SA

Case	Layer thickness (mm)			Fitness value	Value of pressure (Pa)		
	Back	Middle	Front		Fundamental frequency	Second harmonic	Third harmonic
Genetic algorithm							
Case I	0.738	0.186	0.075	9.1×10^{-6}	1102.46	1107.9	1105.1
Case II	0.737693	0.186199	0.074608	4.6×10^{-6}	1108.35	1108.3	1105.32
Particle swarm optimization							
Case I	0.738	0.187	0.074	3.2×10^{-6}	1103.00	1100.50	1100.03
Case II	0.737506	0.186712	0.074281	6.2×10^{-6}	1107.10	1103.65	1102.90
Simulated annealing							
Case I	0.726	0.184	0.089	7.6×10^{-4}	1142.65	1156.07	1106.97
Case II	0.726434	0.184469	0.089096	1.0×10^{-3}	1154.65	1153.55	1102.76

Table 7 Comparison of computational efficiency of GA with PSO and SA

Computational technique	No. of function calls	Fitness value	
		Tol = 1 μm	Tol = 1 nm
Genetic algorithms	135	9.1×10^{-6}	4.00×10^{-6}
Particle swarm optimization	340	3.15×10^{-6}	6.16×10^{-6}
Simulated annealing	300	7.564×10^{-4}	1.035×10^{-6}

impedance in Fig. 4b, the series resonance frequency (f_s) at fundamental frequency is 2.01 MHz. For higher efficiency of transducers in terms of maximum transmission and emission of ultrasonic waves, they are mostly operated at their f_s. The electrical impedance of optimized transducer structure also depicts the uniformity in the first three harmonics. Moreover, from Fig. 4c, it can be observed that uniformity of the harmonics is around $\pm 2.1\%$ as required. Values of layer thickness are demonstrated graphically in Fig. 4a from back to front, while Fig. 4b illustrates a 3D view of the overall fitness values produced during this process against thickness ratios of middle and back layer with respect to front layer. Optimization of multilayer transducer design for various loading media by varying layer thicknesses has also been studied, and results are presented in Table 5.

GA-based results for optimized design of piezo-ceramic transducer under air-coupled acoustic loading are compared with the published results with simulated annealing (Abrar and Cochran 2007) and recent optimization technique of particle swarm optimization (PSO) (Raja et al. 2016b), and presented in Table 6 for comparison. From this table it can be observed that much improved fitness value is achieved by employing GA. Furthermore, in terms of computational efficiency of the optimizer, it can be observed from Table 7 that GA emerges as an optimization technique with faster convergence as it generated results in 135 iterations. PSO algorithm has been implemented to acquire results for multiple layer piezoelectric transducer optimization on the similar pattern as applied in the reported article (Khan et al. 2015b).

The variation of number of layers has also been studied. As demonstrated in Fig. 5a, b, the mechanical output increases while electrical impedance decreases when number of layers is increased from three to five. These graphs are for optimized transducer design with 3, 4, and 5 layers independently; these results of optimization are given in Table 8.

3.1.2 Single crystal: PMN-PT-based multilayer transducer

The characteristics of single-crystal PMN-PT transducer have been explored by optimizing its design using fitness

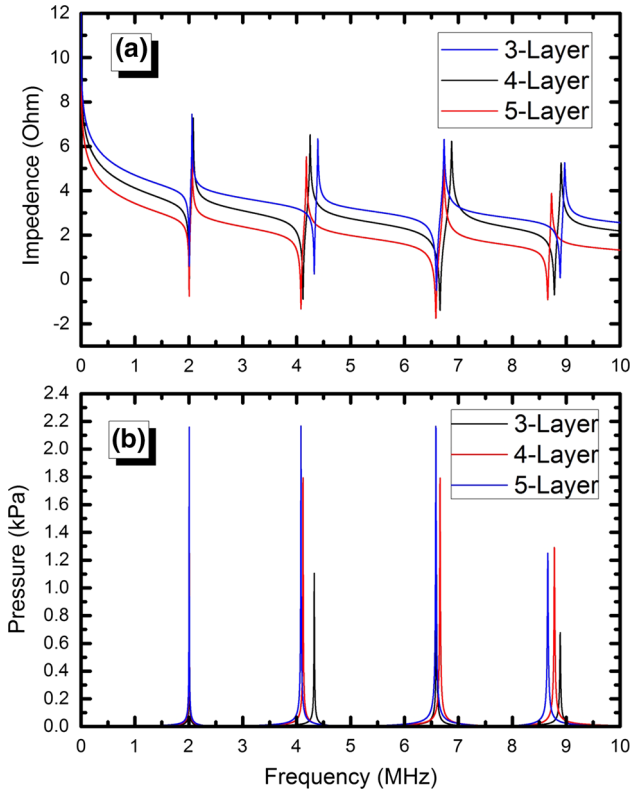

Fig. 5 Comparison of output from optimized transducers with three, four and five layers in terms of **a** impedance magnitude (Ω) and **b** pressure magnitude (kPa)

function as in Eq. 5 under various media. The results of optimization are given in Table 9. For air as acoustic coupling media, the evolutionary plot between fitness value and generations is shown in Fig. 8. Here the optimization process got terminated due to smaller average change in fitness value than the tolerance specified in GA. However, the fitness value has been reduced to such value that can be accepted. The harmonics were generated at 2.01, 4.16 and 6.25 MHz with peak pressure values of 107.39, 103.78 and 106.24 Pa, respectively, as shown in Fig. 6a. Figure 6b–d shows pressure in dB units, impedance magnitude and phase, and evolutionary plot, respectively. As it can be seen the magnitude of impedance is lesser than that of PZT5H; hence, PMN-PT provides improved electrical impedance matching than PZT5H. The thickness values of layers with precision of 1 μm with tolerance of $\pm 0.5\,\mu$m were found to be 0.765, 0.010 and 0.225 mm as presented in Fig. 7.

3.2 Analysis of two-phase piezo-composite transducer

There are different schemes of connectivity of ceramic and polymer materials in composite transducer; in this paper 1–3 connectivity of composite transducer has been considered. In such a connectivity, ceramic is self-connected one dimensionally, while polymer is self-connected three dimensionally (Abrar et al. 2004). The 1–3 piezo connectivity is selected in this paper because such composites have lower acoustic impedance from 8 to 26 MRayl, with high values of coupling coefficient and high bandwidth (Cochran et al. 2011). For piezo-composite structures, the curves between the peaks of pressure magnitude do not go down toward very low amplitude but helps to maintain a broadband in frequency spectrum.

In first part of this section the active material used is PZT5H with passive material CY1301 epoxy. Such composite transducer has been excessively used ranging from underwater SONAR applications to biomedical diagnostic techniques. The material properties of PZT5H are given in Table 4, while the material properties of CY1301/HY1300 epoxy are given in Table 10. In the second part, PMN-PT

Table 8 Results for optimized four-layered and five-layered PZT5H-based transducers

No. of layers	Fitness (10^{-6})	GA variant	Iteration count	Generation count	Layer thickness (mm)				
					(T_1)	(T_2)	(T_3)	(T_4)	(T_5)
4	1.57	GA3	192	9	0.625	0.190	0.047	0.140	–
5	10.8	GA1	153	7	0.597	0.150	0.124	0.022	0.107

Table 9 Optimization data for various loading media

Media (front–back)	Fitness values	Iteration count	Generation count	Layer thickness (mm)			GA variant
				(T_1)	(T_2)	(T_3)	
Air–air	4.6×10^{-4}	535	26	0.765	0.010	0.225	GA1
Water–epoxy	4.0×10^{-6}	194	9	0.265	0.108	0.628	GA5
Air–water	2.0×10^{-6}	135	6	0.261	0.046	0.692	GA5
Water–air	5.6×10^{-6}	236	11	0.652	0.113	0.235	GA1

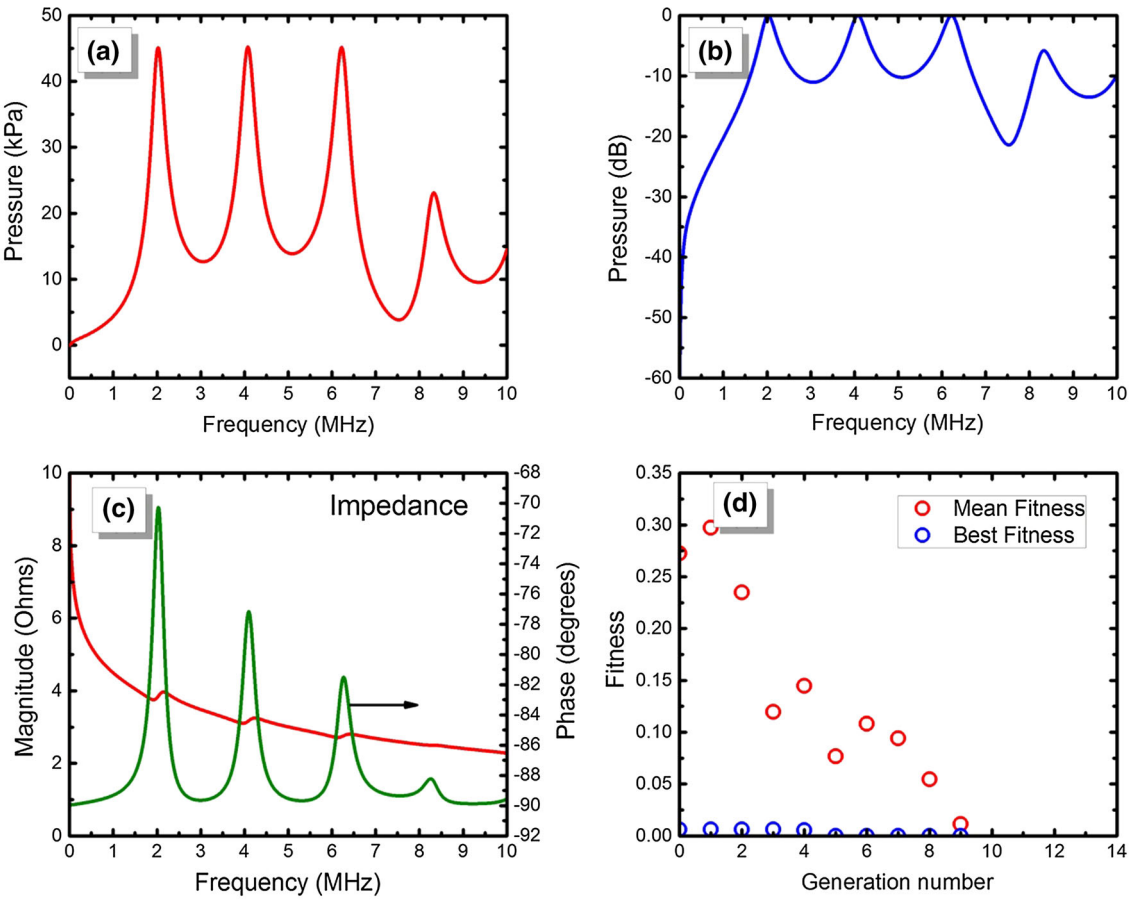

Fig. 6 Optimized three-layered PMN-PT transducer results with water–epoxy acoustic loading using GA. **a** Output pressure (Pa), **b** output pressure (dB), **c** magnitude (Ω) and phase (°) of electrical impedance, and **d** convergence of fitness function

is used as active material and CY1301 epoxy is used as passive material. Such 1–3 composite transducers have vast applications in ultrasonic imaging. The material properties of PMN-PT are mentioned in Table 4.

In this section the characteristics of two different piezo-composite transducers with 1–3 connectivity were presented: PZT5H–epoxy and PMN-PT–epoxy. GAs were used to optimize the design of this transducer. It was found that the optimized design of composite structure of PMN-PT has higher pressure magnitude and lesser electrical impedance than PZT5H composite transducer. Optimization was carried out for both transducers with ceramic volume fraction varying from 30 to 80%, and again GA has proved to be a successful tool for optimization. Piezo-composite transducers have improved sensitivity and bandwidth. This results in their rapid implementation in medical imaging ultrasounds, SONAR and NDT.

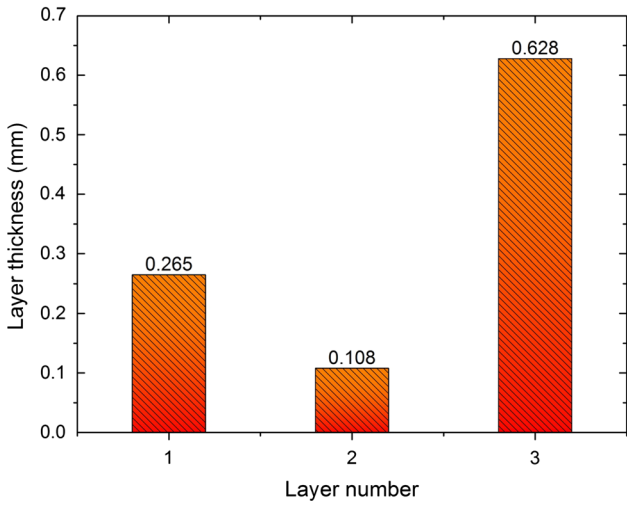

Fig. 7 Resultant optimized thickness values of layers (1 = back layer, 2 = middle layer, and 3 = front layer) of PMN-PT transducer with water–epoxy acoustic loading by GA

Table 10 Summary of physical properties of epoxy

Parameter	Values
Elastic stiffness, C_{33}	9.63×10^9 N m^{-3}
Poisson's ratio	0.35
Relative permittivity at constant strain, ε_R^S	3.5
Density, ρ	1140 kg m^{-3}
Material Attenuation, α	5 dB cm^{-1} at 1 MHz

3.2.1 PZT5H–epoxy piezo-composite as active layers material

The equivalent material properties have been calculated using model given by Smith and Auld (1991). In order to design low-frequency transducer for applications such as SONAR, the total thickness of transducer is kept 3 mm. The characteristics of piezo-composite transducer were studied while varying ceramic volume fraction from 30 to 80% with step of 10%. The simulation results of optimized transducer design for each volume fraction are shown in Table 11. The relative performance among the piezo-composite transducer with different volume fraction was studied by using the following equation:

$$P_i \text{ (dB)} = 20 \times \log_{10}\left(\frac{P_i}{P_{\text{ref}}}\right) \tag{9}$$

where P_i is the pressure calculated at each iteration, while P_{ref} is the maximum pressure value among all iterations. The reference pressure was kept 5920.12, 8389.17, 11504, 13425.8, 15575.8 and 18151.3 Pa for transducer design with ceramic volume fraction as 30, 40, 50, 60, 70 and 80%, respectively. The resulting pressure in decibels and corresponding impedances are plotted as shown in Fig. 8. It can be observed from this figure that while keeping the minima among the harmonics under −3 dB from the peaks of frequency, the ceramic volume fraction from 30 to 40% seems to be appropriate for the broadband transducer design. By increasing the thickness-mode electromechanical coupling constant increases but as ceramic fraction is increased beyond 40%, it starts decreasing (Cochran et al. 2011). Similar behavior is observed in case of electrical impedance.

Table 11 Optimized thicknesses of piezo-composite transducer using PZT5H with varied volume fraction

Volume fraction (%)	Fitness value	No. of function calls	Generation count	Optimized layer thickness (mm)			GA Variant
				(T_1)	(T_2)	(T_3)	
30	1.05E−03	577	28	1.649	0.596	0.785	GA4
40	4.45E−07	178	8	1.663	0.132	1.206	GA4
50	2.02E−03	439	21	1.742	0.011	1.249	GA6
60	5.76E−09	117	5	1.734	0.037	1.230	GA5
70	5.34E−05	578	28	0.749	0.011	2.180	GA4
80	3.58E−06	158	7	0.724	0.168	2.107	GA2

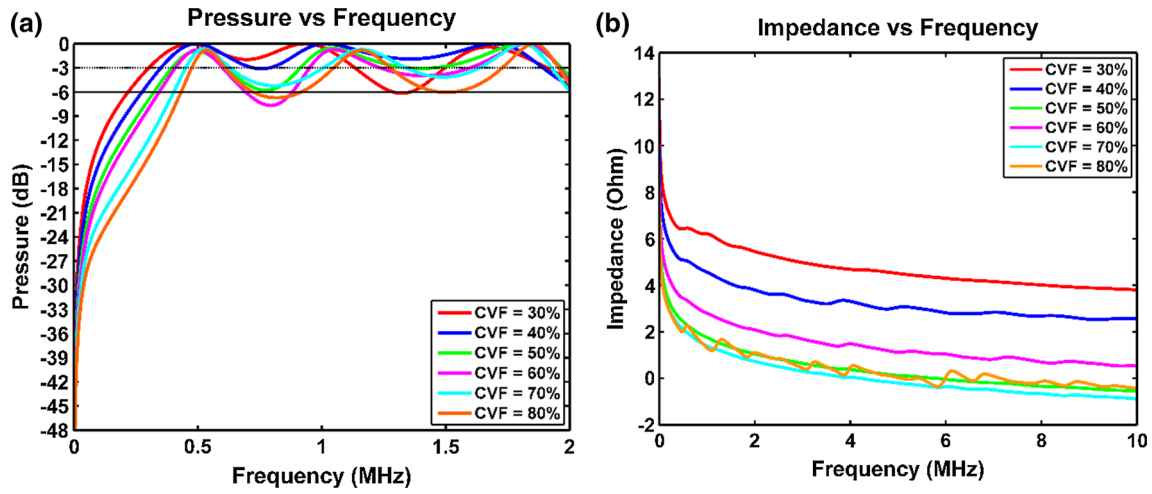

Fig. 8 Output from piezo-composite transducers with varying volume fraction of ceramic PZT5H; **a** pressure output (dB), and **b** magnitude of electrical impedance (Ω)

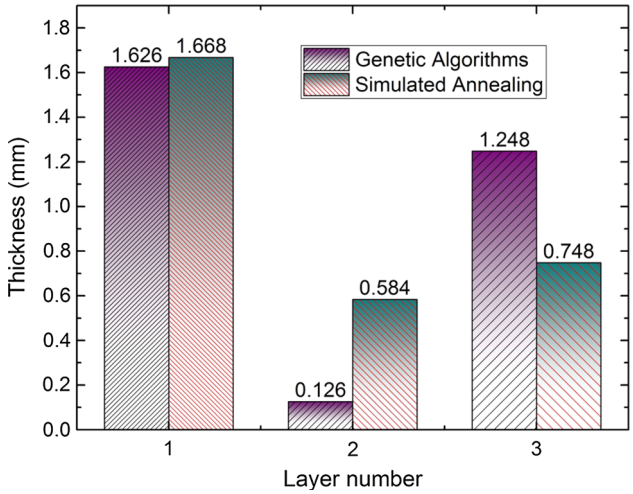

Fig. 9 Comparison of optimized layer thickness values from simulated annealing (Abrar and Cochran 2007) and genetic algorithms

Validation of results

The results of optimization of piezo-composite transducer can be validated by comparing it with already published results (Abrar and Cochran 2007), as well as with PSO and are shown in Table 12. It can be seen that GA produced better results than simulated annealing (SA) in terms of efficiency as fitness value obtained by GA is 1239 times smaller than given by SA. The optimized results are produced after performing 577 iterations with 28 generations using GA variant GA4. The optimized thickness values by GA and SA can be graphically presented in Fig. 9.

Since polymer has lower dielectric constant than ceramic, by increasing the ceramic volume fraction, the overall dielectric constant of composite material increases and hence electrical impedance decreases. This also decreases the mismatch between element and cable and hence increases the sensitivity of probe. However, the bandwidth decreases accordingly. From Fig. 6 it can be seen that the optimized designs of transducer follow this trend.

3.2.2 PMN-PT–epoxy piezo-composite as active layer material

Transducers with 1–3 piezo-composite which composed of single-crystal PMN-PT as an active material with epoxy as a passive material (Cochran et al. 2011) have been optimized, and the results are presented in the form of pressure and impedance output from optimized transducers for various ceramic fractions 30–80% in Fig. 10. Summary of optimized

Table 12 Validation and comparison of composite transducer results of GAs with SA

Case study	Fitness value	Optimized layer thickness value (mm)		
		(T_1)	(T_2)	(T_3)
Simulation results by GAs				
C1	1.38×10^{-6}	1.626	0.126	1.248
Simulation results by PSO				
C1	4.78×10^{-6}	1.625	0.129	1.246
Simulation results by SA (Xu et al. 2015)				
C1	1.71×10^{-3}	1.668	0.584	0.748

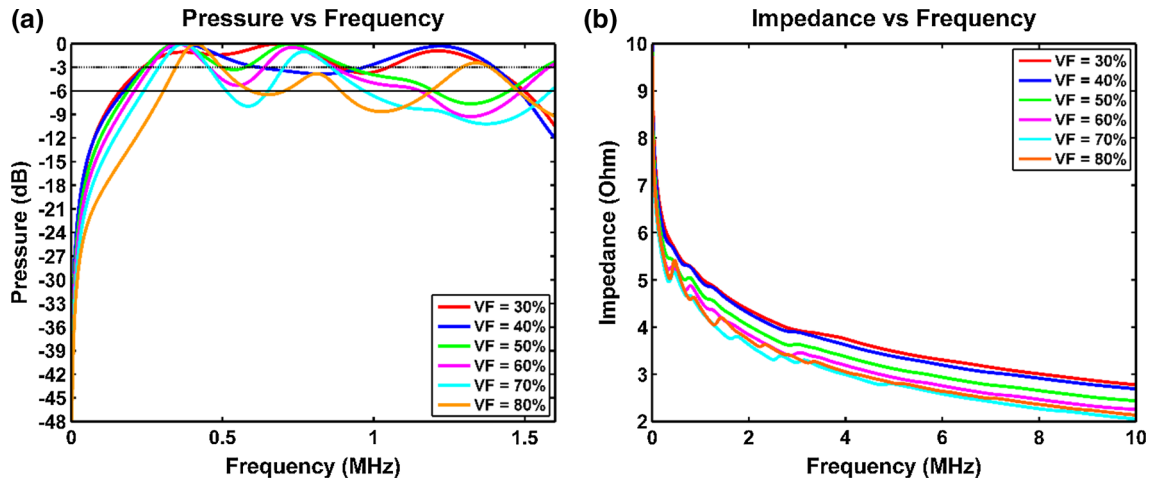

Fig. 10 Output from piezo-composite transducers with varying volume fraction of single-crystal PMN-PT; **a** pressure output (dB), and **b** magnitude of electrical impedance (Ω)

Table 13 Optimized thicknesses of piezo-composite transducer using PMN-PT with varied volume fraction

Volume fraction (%)	Fitness value	No. of function calls	Generation count	Optimized layer thickness (mm)			GA variant
				(T_1)	(T_2)	(T_3)	
30	5.07×10^{-5}	57	2	1.712	0.506	0.781	GA7
40	3.40×10^{-4}	857	42	0.510	0.747	10715	GA3
50	8.85×10^{-5}	179	13	1.643	0.309	1.037	GA11
60	2.06×10^{-3}	1019	50	1.662	0.320	1.048	GA11
70	6.74×10^{-5}	698	34	1.634	0.372	0.998	GA7
80	9.71×10^{-9}	218	10	1.626	0.791	1.583	GA7

thickness values, fitness values, GA variants, etc., are presented in Table 13.

The single crystals have been supposed to have better piezoelectric properties than ceramic materials, and therefore, work had been made to develop signal crystals of PZT. But it was very challenging to grow the crystals and the fabricated crystals were quite small to measure their properties. However, relaxor-based single-crystal, PMN-PT was found to have an enormous piezoelectric constant d_{33}, and coupling factor k_{33} resulting in composite transducer with greater sensitivity and bandwidth.

4 Conclusions

Three-layered piezoelectric transducer structures with piezoceramic material PZT5H and single-crystal PMN-PT have been separately optimized. The results of transducer with piezoelectric material PZT5H have been validated by comparing the results with previously published results. This study shows that the novel use of the standard GA yields better results than SA with less computational cost. Additionally, the other contribution of this work is that optimization of three-layered transducers with single-crystal piezoelectric material PMN-PT alone and in composite form has also been carried out employing GAs. Piezo-composite-based three-layered transducer with PMN-PT is found to be more efficient to convert electrical energy into mechanical (ultrasound) and vice versa. The present study shows that in order to increase the bandwidth and mechanical output of composite transducer, PMN-PT is a preferable piezoelectric material.

Compliance with ethical standards

Conflict of interest All the authors of the manuscript declared that there are no potential conflicts of interest.

References

Abo-Hammour Z, Alsmadi O, Momani S, Arqub OA (2013) A genetic algorithm approach for prediction of linear dynamical systems. Math Probl Eng 2013. https://doi.org/10.1155/2013/831657

Abo-Hammour Z, Arqub OA, Momani S, Shawagfeh N (2014a) Optimization solution of Troesch's and Bratu's problems of ordinary type using novel continuous genetic algorithm. Discrete Dyn Nat Soc 2014. https://doi.org/10.1155/2014/401696

Abo-Hammour Z, Arqub OA, Alsmadi O, Momani S, Alsaedi A (2014b) An optimization algorithm for solving systems of singular boundary value problems. Appl Math Inf Sci 8(6):2809

Abrar A, Cochran S (2007) Mathematical optimization of multilayer piezoelectric devices with nonuniform layers by simulated annealing. IEEE Trans Ultrason Ferroelectr Freq Control 54:1920–1929

Abrar A, Zhang D, Su B, Button TW, Kirk KJ, Cochran S (2004) 1–3 connectivity piezoelectric ceramic-polymer composite transducers made with viscous polymer processing for high frequency ultrasound. Ultrasonics 42(1):479–484

Berlincourt D, Krueger HA, Near C (2000) Properties of Morgan electro ceramic ceramics. In: TP-226. www.morgan-electroceramics.com

Chen Y, Zeng Z, Lu J (2017) Neighborhood rough set reduction with fish swarm algorithm. Soft Comput 21:6907. https://doi.org/10.1007/s00500-016-2393-6

Cochran A, Kirk KJ, Franch PM, Abrar A (2011) Multilayer piezoelectric and polymer ultrawideband ultrasonic transducer. US patent 7,876,027

Cochran S, Parker M, Marin-Franch P (2005) Ultrabroadband single crystal composite transducers for underwater ultrasound. In: Ultrasonics symposium, 2005 IEEE. IEEE, pp 231–234

Dey S, Bhattacharyya S, Maulik U (2014) Chaotic map model-based interference employed in quantum-inspired genetic algorithm to determine the optimum gray level image thresholding. In: Global trends in intelligent computing research and development. IGI Global, pp 68–110

Fu B, Hemsel T, Wallaschek J (2006) Piezoelectric transducer design via multiobjective optimization. Ultrasonics 44:e747–e752

Gao XZ, Ovaska SJ (2002) Genetic algorithm training of Elman neural network in motor fault detection. Neural Comput Appl 11(1):37–44

Hochreiter R, Waldhauser C (2015) Evolving accuracy: a genetic algorithm to improve election night forecasts. Appl Soft Comput 34:606–612

Jurczuk K, Czajkowski M, Kretowski M (2017) Evolutionary induction of a decision tree for large-scale data: a GPU-based approach. Soft Comput 21:7363. https://doi.org/10.1007/s00500-016-2280-1

Khan JA, Raja MAZ, Rashidi MM, Syam MI, Wazwaz AM (2015a) Nature-inspired computing approach for solving non-linear singular Emden–Fowler problem arising in electromagnetic theory. Connect Sci 27(04):377–396. https://doi.org/10.1080/09540091.2015.1092499

Khan JA, Raja MAZ, Syam MI, Tanoli SAK, Awan SE (2015b) Design and application of nature inspired computing approach for nonlinear stiff oscillatory problems. Neural Comput Appl 26(7):1763–1780

Liu T, Gao X, Yuan Q (2017) An improved gradient-based NSGA-II algorithm by a new chaotic map model. Soft Comput 21:7235. https://doi.org/10.1007/s00500-016-2268-x

Lommi A, Massa A, Storti E, Trucco A (2002) Sidelobe reduction in sparse linear arrays by genetic algorithms. Microw Opt Technol Lett 32:194–196

Martin KH, Lindsey BD, Ma J, Lee M, Li S, Foster FS, Jiang X, Dayton PA (2014) Dual-frequency piezoelectric transducers for contrast enhanced ultrasound imaging. Sensors 14(11):20825–20842

Mattiat OE (2013) Ultrasonic transducer materials. Springer, New York

McCall J (2005) Genetic algorithms for modelling and optimisation. J Comput Appl Math 184:205–222

Mokrý P (2016) 100 years of piezoelectric materials in acoustics: from a sonar to active metasurfaces. In: Proceedings of meetings on acoustics 22ICA, vol 28, no 1, p 045008

Panda S, Yegireddy NK (2013) Automatic generation control of multi-area power system using multi-objective non-dominated sorting genetic algorithm-II. Int J Electr Power Energy Syst 53:54–63

Paul PV, Moganarangan N, Kumar SS, Raju R, Vengattaraman T, Dhavachelvan P (2015) Performance analyses over population seeding techniques of the permutation-coded genetic algorithm: an empirical study based on traveling salesman problems. Appl Soft Comput 32:383–402

Powell DJ, Hayward G, Ting RY (1998) Unidimensional modeling of multi-layered piezoelectric transducer structures. IEEE Trans Ultrason Ferroelectr Freq Control 45:667–677

Raja MAZ (2014a) Numerical treatment for boundary value problems of pantograph functional differential equation using computational intelligence algorithms. Appl Soft Comput 24:806–821

Raja MAZ (2014b) Solution of the one-dimensional Bratu equation arising in the fuel ignition model using ANN optimised with PSO and SQP. Connect Sci 26(3):195–214. https://doi.org/10.1080/09540091.2014.907555

Raja MAZ (2014c) Stochastic numerical techniques for solving Troesch's problem. Inf Sci 279:860–873. https://doi.org/10.1016/j.ins.2014.04.036

Raja MAZ, Sabir Z, Mehmood N, Al-Aidarous ES, Khan JA (2015a) Design of stochastic solvers based on genetic algorithms for solving nonlinear equations. Neural Comput Appl 26:1–23

Raja MAZ, Shah FH, Khan AA, Khan NA (2015b) Design of bio-inspired computational intelligence technique for solving steady thin film flow of Johnson–Segalman fluid on vertical cylinder for drainage problem. J Tiawan Inst Chem Eng 60:59–75. https://doi.org/10.1016/j.jtice.2015.10.020

Raja MAZ, Samar R, Alaidarous ES, Shivanian E (2016a) Bio-inspired computing platform for reliable solution of Bratu-type equations arising in the modeling of electrically conducting solids. Appl Math Model. https://doi.org/10.1016/j.apm.2016.01.034

Raja MA, Zahoor AK, Kiani AS, Zameer A (2016b) Memetic computing through bio-inspired heuristics integration with sequential quadratic programming for nonlinear systems arising in different physical models. SpringerPlus 5(1):2063

Rhim, SM, Jung H, Lee K-J (2004) Multilayer PMN-PT single crystal transducer for medical application In: Ultrasonics symposium, 2004 IEEE. IEEE, vol 2, pp 1021–1024

Ru C, Liu X, Sun Y et al (2015) Nanopositioning technologies: fundamentals and applications. Springer, New York

Ruí z A, Ramos A, Emeterio JS (2004) Estimation of some transducer parameters in a broadband piezoelectric transmitter by using an artificial intelligence technique. Ultrasonics 42:459–463

Smith WA, Auld B (1991) Modeling 1–3 composite piezoelectrics: thickness-mode oscillations. IEEE Trans Ultrason Ferroelectr Freq Control 38:40–47

Soloviev AN, Oganesyan PA, Lupeiko TG, Kirillova EV, Chang SH, Yang CD (2016) Modeling of non-uniform polarization for multi-layered piezoelectric transducer for energy harvesting devices. In: Parinov I, Chang SH, Topolov V (eds) Advanced materials. Springer, Cham, pp 651–658

Wu Z, Abrar A, McRobbie G, Gallagher S, Cochran S (2003) Implementation of multilayer ultrasonic transducer structures with optimized non-uniform layer thicknesses. In: 2003 IEEE symposium on ultrasonics. IEEE, pp 1292–1295

Xu Y, Xu D, Qu J, Cheng X, Jiao H, Huang S (2015) Concrete crack damage location based on piezoelectric composite acoustic emission sensor. In: Shen G, Wu Z, Zhang J (eds) Advances in acoustic emission technology. Springer, New York, pp 347–353

Zameer A, Mirza SM, Mirza NM (2014) Core loading pattern optimization of a typical two-loop 300MWe PWR using Simulated Annealing (SA), novel crossover Genetic Algorithms (GA) and hybrid GA (SA) schemes. Ann Nucl Energy 65:122–131